Available online at www.sciencedirect.com

SCIENCE DIRECT

Thin Solid Films 472 (2005) 144–149

www.elsevier.com/locate/tsf

Manganese distribution in ferromagnetic gallium manganese nitride epitaxial film grown by plasma enhanced molecular beam epitaxy

Joonyeon Chang[a,*], Gyeungho Kim[b], Woo-Young Lee[c], Jae-Min Myoung[c]

[a]Nano Device Research Center, Korea Institute of Science and Technology, P.O. Box 131, Cheongryang, Seoul 130-650, Korea
[b]Nano-Materials Research Center, Korea Institute of Science and Technology, P.O. Box 131, Cheongryang, Seoul 130-650, Korea
[c]Department of Materials Science and Engineering, Yonsei University, 134 Shinchon-Dong, Seoul 120-749, Korea

Received 20 June 2004; received in revised form 21 June 2004; accepted 23 June 2004
Available online 12 August 2004

Abstract

Systematic transmission electron microscopy (TEM) study was performed to determine the change in lattice parameter of epitaxial Mn-doped GaN films with low Mn contents (0.06–0.5 at.%) grown by plasma-enhanced molecular beam epitaxy (PEMBE) by which added Mn distribution can be investigated. Secondary ion mass spectroscopy (SIMS) reveals that the Mn profiles for the films are uniform throughout the entire thickness range of 0.7–1.0 μm with no appreciable segregation. The lattice parameter for the plasma-enhanced molecular beam epitaxy grown GaMnN is found to be a=0.31865 nm, larger than those for the metal organic chemical vapor deposition grown GaN used as a substrate and plasma-enhanced molecular beam epitaxy grown GaN on metal organic chemical vapor deposition GaN, reflecting the expansion of unit lattice due to Mn ion substitution for Ga ion in the wurtzite $(Ga_xMn_{1-x})N$ structure. Lattice parameter measurement is believed to give useful information on the crystalline quality of $(Ga_xMn_{1-x})N$ structure grown by plasma-enhanced molecular beam epitaxy.

PACS: 71.20.Nr; 75.50.Pp; 61.16.Bg
Keywords: Gallium nitride (GaN); Ferromagnetism; (Ga,Mn)N; Lattice parameter; Convergent beam electron diffraction (CBED)

1. Introduction

In recent years, ferromagnetic semiconductors have drawn great interests due to potential applications in spintronics, in which the spin of charge carriers (electrons or holes) may lead to fundamentally novel functionality with respect to conventional semiconductor devices [1,2].

In spite of the potential attraction, low solubility of magnetic element (Mn) in the compounds such as GaAs and GaN makes it difficult to fabricate ferromagnetic III–V semiconductors and is known to be a major obstacle to overcome for the practical applications [1]. When a high concentration of magnetic element is introduced in excess of the solubility limit, formation of a secondary phase occurs if the conditions are in near equilibrium. Since the magnetic effects are roughly proportional to the concentration of the magnetic ions, it is very important to suppress the formation of the secondary phase containing Mn [3,4]. In addition, there is a need to accurately determine the concentration of Mn doped into a semiconductor.

For wurtzite (Ga,Mn)N fabricated by low temperature molecular beam epitaxial (MBE) growth that allows to grow (Ga,Mn)N far from equilibrium to prevent the formation of Mn secondary phase [5], it is essential to evaluate the crystalline quality of grown (Ga,Mn)N thereby we can judge the magnetic properties of Mn-doped GaN originated from Mn ion substituting for Ga. With a difficulty in growing nitride with low temperature MBE, only a few papers have been reported to date [4–7]. Furthermore, most of works on GaMnN largely rely on the X-ray diffraction technique to determine Mn distribution. This technique only allows average information on the crystalline phase and no study

* Corresponding author. Tel.: +82 2 958 6822; fax: +82 2 958 6851.
E-mail address: presto@kist.re.kr (J. Chang).

0040-6090/$ - see front matter © 2004 Elsevier B.V. All rights reserved.
doi:10.1016/j.tsf.2004.06.144

employing convergent beam electron diffraction (CBED) method in transmission electron microscopy (TEM) to evaluate the local lattice parameter change in Mn-doped GaN has ever made. CBED is well known to be very powerful technique to characterize the multiphase materials by providing the local lattice parameter change and also applied in epitaxial GaN layers grown on various substrate materials and processes [8,9].

In this paper, we examine the wurtzite (Ga,Mn)N solid solution by comparing the lattice parameters of plasma-enhanced molecular beam epitaxy (PEMBE) grown GaMnN, metal organic chemical vapor deposition (MOCVD) grown GaN, PEMBE grown GaN on MOCVD GaN with a standard GaN sample as a reference. Accurate measurement of lattice parameter was performed using CBED in TEM, which was employed to obtain high order Laue zone (HOLZ) pattern. The measured lattice parameter variation strongly indicates that the ferromagnetic ordering of (Ga,Mn)N is mainly due to Mn element substitution for Ga.

2. Experimental

The Mn-doped GaN films were grown by PEMBE system under ultrahigh vacuum conditions (UHV) with a base pressure of ~8×10^{-10} Torr. High-purity Ga and Mn metals (6N and 5N5, respectively) were used as source materials. As a nitrogen source, high-purity (6N) nitrogen gas was supplied through an RF plasma source. For the epitaxial growth, 2-μm-thick GaN templates on sapphire (0001) were prepared as substrates by low-pressure MOCVD with the conventional two-step procedure, consisting of low-temperature growth of a 40-nm-thick buffer layer and high temperature growth of overlayer [10] prior to the deposition of the Mn-doped GaN layers. The (Ga,Mn)N films were grown at various Mn cell temperatures ranging from 600 to 700 °C and at a fixed Ga-cell temperature of 1000 °C. A PHI 7200 TOF-SIMS instrument was used in the SIMS measurements. A beam of 8 keV Cs^+ ions of ~50 nA was incident on the GaMnN film at an incident angle 60°. The signals were detected for depth profiling of Ga, Mn and N, respectively. As-grown ($Ga_{1-x}Mn_x$)N films with low Mn content (x=0.06–0.5%) was revealed to show n-type conductivity and ferromagnetism (M_s=0.3–1.9 emu/cm^3, H_c=45–115 Oe) with Curie temperature in the range 550–700 K [7].

TEM observation was performed with the TEM (Philips CM 30) operated at 200 kV. The CBED technique was used to measure the lattice parameter change with the addition of Mn. Cross-sectional TEM specimen were made using a Ti grid and bonded with epoxy (Gatan, G-1). Epoxy cured specimens were ground to 100 μm by mechanical polishing and to 20 μm by dimple grinder (Gatan, Model 656). Further thinning was performed by ion miller (Gatan Duomil Model 600) operated with an accelerating voltage of 6 kV and gun current of 0.5 mA under 13° milling angle with 80° single sector control mode. HOLZ patterns were obtained on the zone axis of [$\bar{2}$201] of GaN with convergent beam angle of 2 nm^{-1}. The 200-μm-thick GaN grown on sapphire substrate by hydride vapor phase epitaxy (HVPE) and removed from the sapphire to eliminate mismatch strain was chosen as the standard sample for comparison. HOLZ pattern under the same TEM condition was obtained on the standard sample. Simulated HOLZ pattern was obtained by using JEMS (Java for EMS) program, which simulates the HOLZ pattern using dynamic calculation. Lattice parameter was determined by comparing the simulated and measured ratio of the distances between intersection point 1 of ($\bar{5}$,$\bar{3}$,$\bar{3}$) and (3,5,$\bar{3}$) line, point 2 intersection of (1,$\bar{4}$,11) and (4,$\bar{1}$,11), point 3 intersection of ($\bar{5}$,0,$\bar{9}$) and (0,5,$\bar{9}$), point 4 intersection of (1,$\bar{4}$,11) and ($\bar{5}$,$\bar{3}$,$\bar{3}$), point 5 intersection of (4,$\bar{1}$,11) and (3,5,$\bar{3}$), point 6 intersection of ($\bar{5}$,$\bar{3}$,$\bar{3}$) and (0,5,$\bar{9}$), and point 7 intersection of (3,5,$\bar{3}$) and ($\bar{5}$,0,$\bar{9}$) as shown in Fig. 3.

3. Results and discussion

Fig. 1 shows the depth profiles of Mn, Ga and N for the Mn-doped GaN films grown with Mn cell temperatures of 650 and 670 °C, obtained by secondary ion mass spectroscopy (SIMS). The Mn profiles were found to be uniform for the films throughout the entire thickness in the range 0.7–1.0 μm with no appreciable segregation. Mn concentration appears to increase with increasing Mn cell temperature. In the present work, Mn concentration was estimated from calculations using the total magnetic moment, provided each Mn atom has the theoretical magnetic moment of $3\mu_B$ [11], since quantitative determination is difficult due to very low Mn concentration (x=0.0006–0.005).

Fig. 2 shows the cross-sectional TEM micrograph of (Ga,Mn)N/MOCVD GaN grown on a sapphire substrate. (Ga,Mn)N epitaxial film of 0.7 μm in thickness was

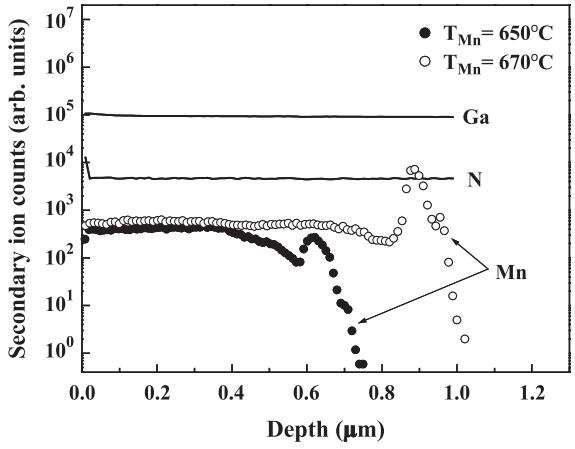

Fig. 1. The depth profiles of Mn, Ga and N for the (Ga,Mn)N films grown with Mn cell temperatures of 650 and 670 °C obtained by secondary ion mass spectroscopy.

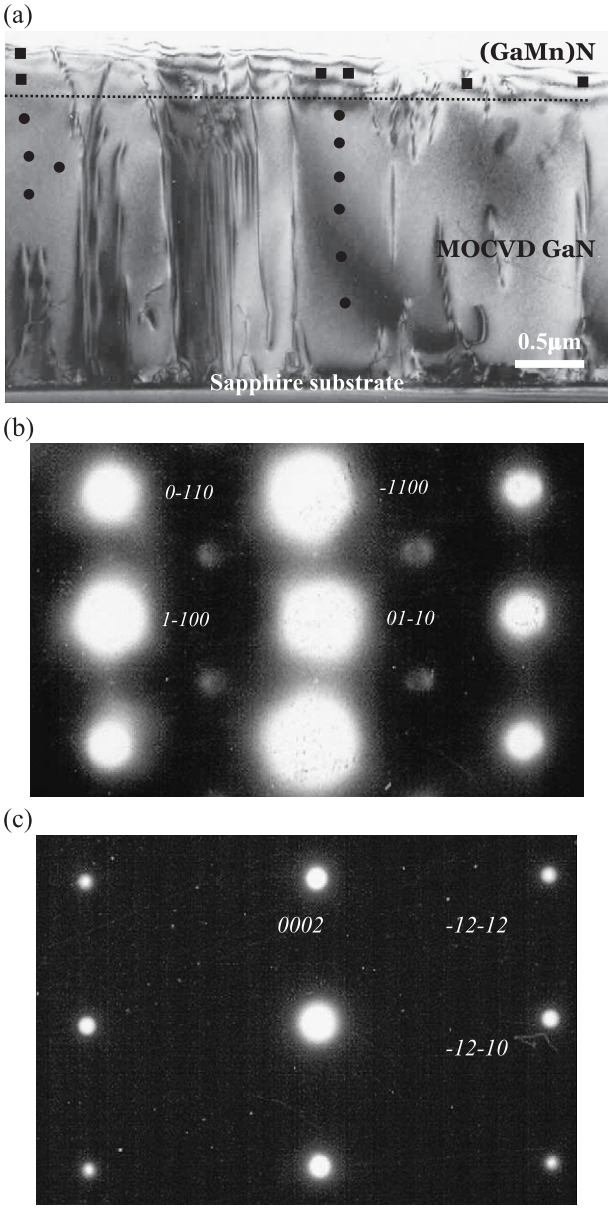

Fig. 2. (a) Cross-sectional TEM image of (Ga,Mn)N (upper) grown on MOCVD GaN (lower) circle and square indicate points where HOLZ patterns are obtained. (b) Selected area diffraction (SAD) pattern from (GaMn)N. Additional diffraction spots (indexed by italic) indicates the twin spots of $(01\bar{1}2)$ twinning in the $[01\bar{1}0]$ matrix. (c) SAD pattern from lower MOCVD GaN on zone axis $B=[10\bar{1}0]$ showing no additional spots.

deposited on top of 2-μm-thick MOCVD GaN. Large numbers of threading dislocations initiated at the interface between the substrate and MOCVD GaN propagate vertically to (Ga,Mn)N, which are developed to accommodate the large lattice mismatch of 16% with the sapphire substrate. Lack of good lattice match for epitaxial growth of GaN on sapphire results in high dislocation density. Comparing the electron diffraction patterns from (Ga,Mn)N (upper) and MOCVD GaN (lower), the additional diffraction spots (indexed in *italic* in the figure) can be found in (Ga,Mn)N, which are extra *hkil* diffraction spots in the zone axis of $B=[01\bar{1}0]$. The appearance of such the extra diffraction is known to be a result from a single twin orientation of the closed packed hexagonal matrix [12]. According to Reed et al. [4], these additional reflections in the (Ga,Mn)N is considered as a kind of evidences of solid solution (Ga,Mn)N structure together with forbidden peak of (0001) in X-ray diffraction.

In order to obtain a solid evidence of Mn distribution in (Ga,Mn)N solid solution, we tried to evaluate the lattice parameter of (Ga,Mn)N by comparing the HOLZ patterns. The evaluation was also performed on MOCVD GaN, on Mn-undoped GaN grown on MOCVD GaN and the standard GaN for comparison. The zone axis chosen for the analysis was $[\bar{2}201]$ of GaN, which has a mirror symmetry with sharp HOLZ lines that are observable at room temperature. To reduce the errors in the measurements, distances of HOLZ line intersection points were measured and their ratios were calculated and compared. It has been well documented that the absolute value of lattice parameter can be obtained by tilting the crystal away from the zone-axis center, quantifying the HOLZ pattern using the distance between HOLZ line intersections, measuring the distance digitally by computer, defining a best-fit parameter and using many HOLZ lines with an optimization routine to find the best fit [13].

Simulated and experimental $[\bar{2}201]$ HOLZ patterns are given in Fig. 3 showing indexed HOLZ lines and intersection points used in the measurement. The distances α, β, γ and δ were measured to calculate the ratios α/β and γ/δ. The distance between two points 1–2 was defined as α and, similarly, distance 1–3 as β, distance 4–5 as γ and the distance between 6 and 7 as δ. Note that the value of α/β is sensitive to the lattice parameter change of GaN in the a-axis, while γ/δ value reflects the change perpendicular to the interface. Simulation of HOLZ patterns with lattice parameter change indicated that the ratios α/β and γ/δ are inversely proportional to the a-axis lattice parameter. The opposite trend was observed with the c-axis parameter variation, i.e., both ratios increased with increasing c-axis lattice parameter at constant a-axis value. From the simulation of HOLZ patterns, it is difficult to obtain quantitative values of lattice parameters in wurtzite structure of GaN, which has two independent lattice parameters (a- and c-axes). Basically, Mn substitution for Ga in GaN superstructure essentially results in change in lattice parameter based on relative magnitude between Ga–N and Mn–N bonding strength as well as the fraction of added Mn contents, which is known to Vegard's law. Since this substitution can be expected to change the both a- and c-axes independently, it is reasonable to measure both values. However, the difficulty of simulation limits this job so that change in a was simulated and measured under the corresponding change of c in the study. That is, the unit cell volume invariance was used to simulate the HOLZ pattern. The change in a is regarded as a direct evidence of Mn substitution for Ga with which crystalline quality of Mn-doped GaN can be determined.

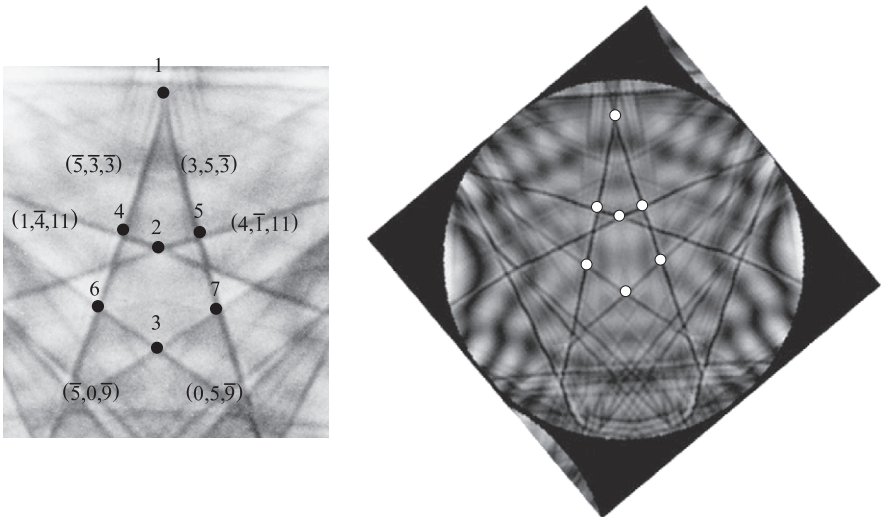

Fig. 3. Comparison of observed and simulated GaN [2̄201] HOLZ patterns, (a) experimental pattern with indexed HOLZ lines used, (b) simulated HOLZ pattern from dynamic simulation method.

Different extents of distortion of HOLZ lines were found in (Ga,Mn)N (b), MOCVD GaN (c) and Mn-undoped GaN grown on MOCVD GaN (d) as shown in Fig. 4. Compared to the HOLZ pattern of the standard sample (a), those of (Ga,Mn)N and MOCVD GaN show a shifted HOLZ line indicating the change in lattice parameter happens. It may give a reasonable clue to understand the distribution of Mn in GaN structure. The ratios were measured from the HOLZ patterns to evaluate the change in a. If Mn can substitute for Ga, the lattice parameter can be expected to increase based on the same explanation applied to (Ga,Mn)As system [3].

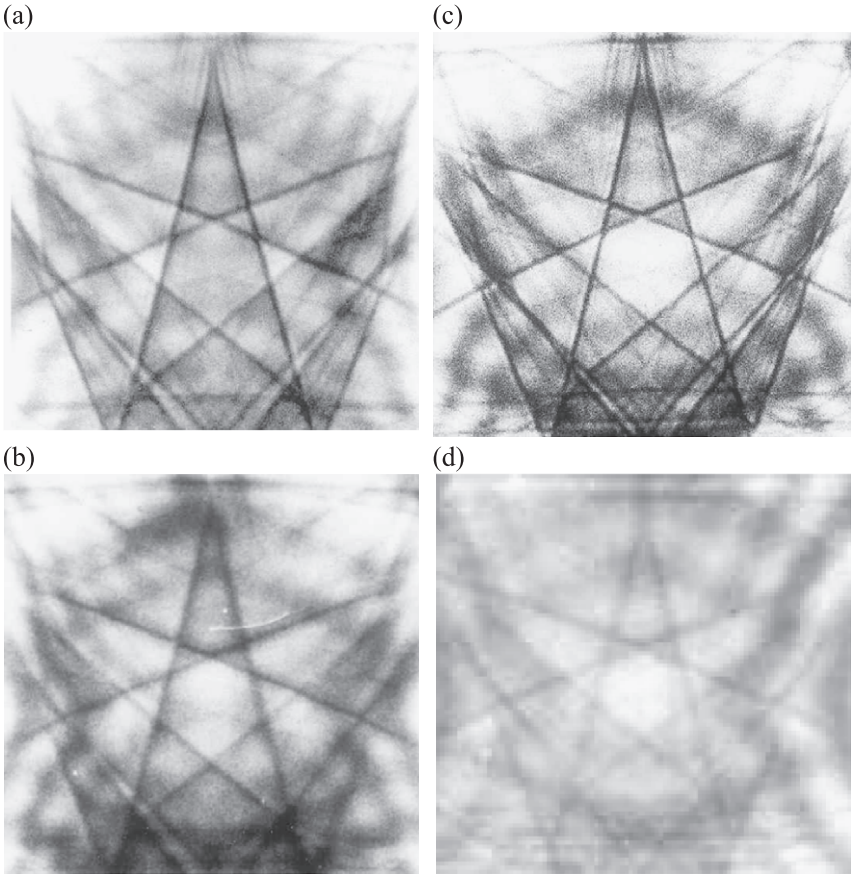

Fig. 4. [2̄201] zone axis HOLZ patterns obtained from various GaN at 200kV. (a) Standard GaN sample with no mismatch strain (b) (Ga,Mn)N on top of MOCVD GaN. (c) MOCVD GaN as a substrate for (Ga,Mn)N growth. (d) Mn-undoped GaN on top of MOCVD GaN.

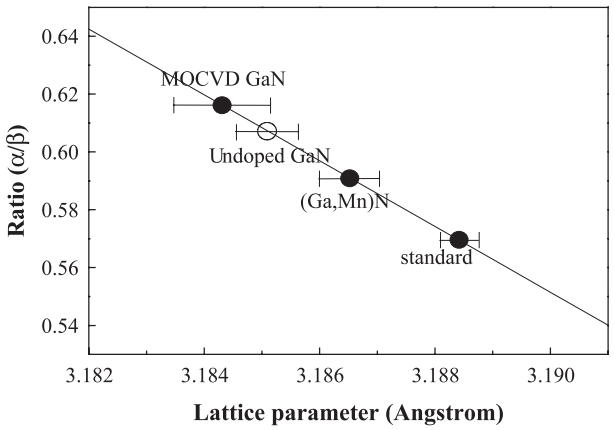

Fig. 5. Distance ratios measured from the HOLZ patterns and corresponding lattice parameters (a) of various GaN samples.

Fig. 5 shows results of the lattice parameter measurement of each sample. The average value of ratios obtained from the standard GaN sample is 0.56988, corresponding to a=0.31884 nm, which is off only 0.01% to the standard lattice parameter of 0.31880 nm used for the simulation. This shows that the measurement using HOLZ pattern is very reliable to evaluate the lattice parameter. According to the literature [13], it is possible to measure the absolute value of lattice parameters to about 0.015%. The major factor limiting the accuracy of lattice parameter measurement by HOLZ lines is dynamical effects. By avoiding the zone axis center, especially, low-index zone axis centers, dynamical effects can be reduced by an order of magnitude or more. Thus, the accuracy of the lattice parameters is increased by a similar factor. Since there is a 16% lattice misfit at the interface of sapphire and GaN, contraction of GaN along the a-axis is expected to accommodate the misfit strain. In the case of MOCVD GaN directly deposited on a sapphire substrate, a is calculated to 0.31843 nm, which shrinks almost 0.1286% compared to the standard sample as expected. By the contrast, small increase in the a of 0.31865nm is found in the (Ga,Mn)N, even though it does not reach the standard value of 0.31880 nm. For (Ga,Mn)N, the same contraction should be applied owing to the lattice mismatch with sapphire although it grows on top of MOCVD GaN. Nevertheless, it is believed that increase in the lattice parameter a observed in (Ga,Mn)N strongly indicates the substitution of Mn for Ga in wurtzite GaN superlattice.

To elucidate the source of the increase, we also attempted to measure the lattice parameter a in Mn-undoped GaN grown on the MOCVD GaN, which is the same as used for (Ga,Mn)N growth. Open circles in Fig. 5 showing the lattice parameter a of Mn-undoped GaN is very close to that of the MOCVD GaN, implying that the increase in the a observed in (Ga,Mn)N is entirely induced by the Mn substitution for Ga. That is, this increase is not caused by the release of the misfit strain but by the solid solution of (Ga,Mn)N structure.

Increase in lattice parameter of GaN can be explained by the existence of Mn solutes. Some recent publications strongly confirm that majority Mn atoms are incorporated substitutionally on the Ga sublattice sites resulting in increase in lattice parameter of GaN [14,15]. Lattice change is directly used to evaluate the Mn concentration, which is believed to be difficult owing to small amount of adding Mn concentration as well as a lack of applicable measurements. Since the lattice strain of undoped GaN is −0.094%, which is entirely due to lattice mismatch strain, this can be used as a reference value. The difference between Mn-doped GaN and undoped GaN, 0.015% increase in lattice parameter is attributed to the incorporation of doped Mn solutes in GaN.

Unfortunately, no known formula exists between the lattice parameters and concentration of Mn solute in GaN structure and direct calculation of Mn concentration is currently in trouble with the obtained lattice strain.

4. Conclusion

(Ga,Mn)N epitaxial film was successfully grown on MOCVD GaN as a substrate by plasma enhanced molecular beam epitaxy. The film shows strong ferromagnetic ordering at room temperature. Uniform Mn profiles for the films are observed throughout the entire film thickness in the range 0.7–1.0 μm with no appreciable segregation from SIMS study. The analytical TEM study reveals that the lattice parameter for the (Ga,Mn)N increases to a=0.31865 nm, which is larger than those for the MOCVD-grown GaN and Mn-undoped GaN, reflecting the expansion of a due to Mn ion substitution for Ga ion in the wurtzite (Ga,Mn)N structure. Lattice parameter measurement using CBED is an efficient method to investigate the microstructure of diluted magnetic semiconductor, which has been known to be difficult to form complete solid solution structure due to low solubility of magnetic ions.

Acknowledgements

This work was supported by KIST Vision 21 program.

References

[1] H. Ohno, Science 281 (1998) 951.
[2] S.A. Wolf, D.D. Awschalom, R.A. Buhrman, J.M. Daughton, S. Molnar, M.L. Roukes, A.Y. Chtchelkanova, D.M. Treger, Science 294 (2001) 1488.
[3] H. Ohno, A. Shen, F. Matsukura, A. Oiwa, A. Endo, S. Katsumoto, Y. Iye, Appl. Phys. Lett. 69 (1996) 363.
[4] M.L. Reed, N.A. El-Masry, H.H. Stadelmaier, M.K. Ritums, M.J. Reed, C.A. Parker, J.C. Roberts, S.M. Bedair, Appl. Phys. Lett. 79 (2002) 3473.
[5] S. Sonoda, S. Shimizu, T. Sasaki, Y. Yamamoto, H. Hori, J. Cryst. Growth 237–239 (2002) 1358.

[6] G.T. Thaler, M.E. Overberg, B. Gila, R. Frazier, C.R. Abernathy, S.J. Pearton, J.S. Lee, S.Y. Lee, Y.D. Park, Z.G. Khim, J. Kim, F. Ren, Appl. Phys. Lett. 80 (2002) 3964.
[7] K.S. Huh, M.H. Ham, J.M. Myoung, J.M. Lee, K.I. Lee, J.Y. Chang, S.H. Han, H.J. Kim, W.Y. Lee, Jpn. J. Appl. Phys 41 (2002) L1069.
[8] V. Randle, I. Barker, B. Ralph, J. Electron Microscopy Tech. B 13 (1989) 51.
[9] H.J. Kim, D.J. Byun, G.H. Kim, D.W. Kum, J. Appl. Phys 87 (2000) 7940.
[10] A. Sakai, H. Sunakwaw, A. Usui, Appl. Phys. Lett. 71 (1997) 2259.
[11] Y.D. Park, A.T. Hanbicki, S.C. Erwin, C.S. Hellberg, J.M. Sullivan, J.E. Mattson, T.F. Ambrose, A. Wilson, G. Spanos, B.T. Jonker, Science 295 (2002) 651.
[12] W. Edington, Monographs in Practical Electron Microscopy in Materials Science, N.V. Philips' Gloeilampenfabrieken, Eindhoven 2 (1975) 52.
[13] J.M. Zuo, Ultramicroscopy 41 (1992) 211.
[14] Y.L. Soo, G. Kioseoglou, S. Kim, S. Huang, Y.H. Kao, S. Kuwabara, S. Owa, T. Kondo, H. Munekata, Appl. Phys. Lett. 79 (2001) 3926.
[15] F. Zhang, N. Chen, X. Liu, S. Yang, C. Chai, J. Cryst. Growth 262 (2004) 287.